



Research paper

Boron-based metallocene-like molecules and nanowires: A computational study

Xiaojie Fu^a, Di Wang^a, Xiaolin Song^a, Xingfa Gao^a, Joonkyung Jang^{b,*}, Xuejiao J. Gao^{a,*}

^a College of Chemistry and Chemical Engineering, Jiangxi Normal University, Nanchang 330022, China

^b Department of Nanoenergy Engineering, Pusan National University, Busan 46241, South Korea

HIGHLIGHTS

- The Lewis-base stabilized borylenes and boryls is applied for molecule and material design.
- $B_5(CO)_5$ is the η^5 -ligand with stronger bonding affinity with Mn and Fe than the traditional cyclopentadiene.
- The designed nanowire $[VB_5(CO)_5FeB_5(CO)_5]_\infty$ is predicated as an organic half-metal.

ABSTRACT

The Lewis base stabilized borylenes and boryls are used to construct one dimension nanowires. Using the Lewis base (L) to coordinate sp^2 borons, we constructed $B_5L_5^-$ cyclic compounds with six π -electrons. Then, using B_5L_5 and transition metals as building units, we further constructed half-sandwich and sandwich compounds. We found that the $B_5(CO)_5$ is the η^5 -ligand with stronger bonding affinity with Mn and Fe than the traditional cyclopentadiene. The calculated electronic band structures suggested that the constructed nanowire $[VB_5(CO)_5FeB_5(CO)_5]_\infty$ is an organic half-metal. The results may cast light on the future synthesis of boron-based metallocene-like molecules.

1. Introduction

Boron has three valence electrons but four valence orbitals and thus is electron deficient. The bonding model **a** is well-known for sp^2 hybridized borons, which successfully explains the chemical properties of many organoboron compounds like borane BH_3 . Interestingly, experimental and theoretical studies in the past decades have unambiguously demonstrated the stable existence of different boron compounds, where the chemistries of borons are better explained with models **b** and **c** (Fig. 1) [1–8]. For example, Robinson and co-workers [9] have synthesized the Lewis based stabilized diborene, in which the B atoms form the B = B double bond and adopt the bonding configuration **b**. In 2011, Bertrand and co-workers first synthesized tricoordinate organoboron where the B atoms adopt the configuration **c** [10]. Braunschweig and co-workers [11] then synthesized Lewis base stabilized monoborenes, where the B atoms also adopt the configuration **c**. One of the main differences for models **a**, **b**, and **c** exists in the p_z orbital occupation numbers, where $n(p_z) = 0, 1, \text{ and } 2$, respectively. The $n(p_z)$ values are equal to the numbers of donor–acceptor bonds made by the B sp^2 orbitals and the base ligands L [$n(L \rightarrow sp^2) = 0, 1, \text{ and } 2$, respectively]. Such base stabilized borylenes and boryls have opened a broad

opportunity to design and synthesize novel boron molecules [12,13], which have potentials in applications like catalysis [3,14–16] and low-temperature nitrogen fixation [17].

Recently, Gao *et al.* have computationally studied the two-dimensional (2D) frameworks containing the c-type borons, suggesting the possibility to use the based stabilized borylenes and boryls for material design [18]. On the other hand, Tai and Nguyen have reported that the b-type borons can form stable molecules containing monocyclic B_n ($n = 3–6$) rings [7]. Inspired by these results, we hereby study the possibility to use the B_n rings as the η^n -ligands to form metallocene-like molecules with transition metals M, and further construct one dimensional (1D) nanowires based on the sandwich metallocene-like structures. We report that the B_nL_n rings have the capability as the η^n -ligands to bind with transition metals to form metallocene-like molecules, and that the $(MB_5L_5)_\infty$ nanowires have metallic, semiconducting, and half-metallic electronic structures.

2. Methods

For 0D molecular, all geometries were optimized using the B3LYP, M062X and PBE functional with the 6-31G(d, p) basis sets [19,20] for

* Corresponding authors.

E-mail addresses: jkjang@pusan.ac.kr (J. Jang), gaoxj@jxnu.edu.cn (X.J. Gao).

<https://doi.org/10.1016/j.cplett.2020.137336>

Received 1 February 2020; Received in revised form 8 March 2020; Accepted 9 March 2020

Available online 10 March 2020

0009-2614/ © 2020 Published by Elsevier B.V.

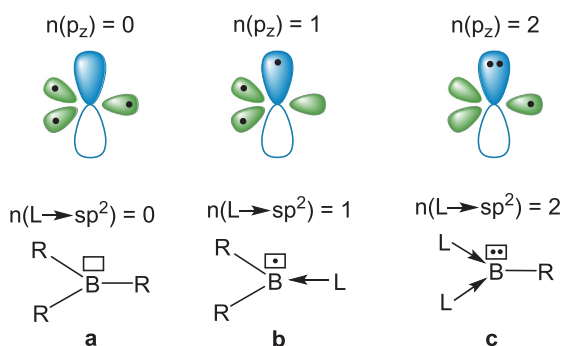


Fig. 1. The electronic structure of boron compounds and the binding between boron complex and Lewis basis L.

light atoms and the SDD basis sets and pseudopotential [21,22] for metals, as implemented in the GAUSSIAN 09 package [23]. The dispersion is considered. DFT-D3(BJ) is applied with B3LYP and PBE functional and DFT-D3 is applied with M062X functional. Frequency analyses were conducted at the same level of theory to ensure that there is no imaginary frequency for the stationary point on the potential energy surface. The ETS-NOCV analysis [24–26] was performed to calculate the orbital interaction contributions to the bonds between two fragments in a molecule. These calculations were performed using the BP86 [27–29] exchange–correlation functional with the TZ2P basis sets, as implemented in the ADF (2014.10) package [30].

For 1D nanowire, geometry optimization, projected density of states (PDOS) and band structure calculation were performed using the VASP program [31,32]. GGA + U method [33], a plane-wave cutoff of 520 eV, a Gaussian smearing of 0.05 eV, an energy convergence criterion of 10^{-5} eV and a force convergence criterion of 0.02 eV/Å were adopted. The effective U values for metals are listed in Table S2 in the supporting information (SI). For the geometry optimization, the $(7 \times 1 \times 1)$ Monkhorst–Pack [34] mesh k-points were used and for the PDOS and band structure calculations, the $(11 \times 1 \times 1)$ k-points were used. To distinctively set the magnetism states, ferromagnetic (FM) and antiferromagnetic (AFM), for the 1D nanowire, a supercell containing 4 unit cells were used.

3. Results and discussion

3.1. Monocyclic $B_5L_5^-$ anions

$[B_3(NHC)_3]^+$, $[B_3(NN)_3]^+$ and $[B_3(CO)_3]^+$ have been reported and featured as the smallest π -aromatic species B_3^+ [7,8]. Although the heavier group-13 homologues $[Ga_3R_3][M_2]$ ($M = Na, K$; R = bulky, aryl) and $[E_3H_3]^{2-}$ ($E = B, Al, Ga$) have been synthesized [35–37], the base stabilized boron compounds $B_3L_3^+$ are not observed yet. Here, we studied the structures and B–L bonding strengths for six $B_5L_5^-$ compounds **1a**–**1f**, where the L varies from A through F (Fig. 2). According to the knowledge recently established for Lewis base stabilized borylenes and boryls, the reasonable bonding model for these compounds is shown in Fig. 2a. All the B atoms are sp^2 hybridized. Each B atom uses two of its sp^2 atomic orbitals to form the electron-sharing σ -bonds with its neighbouring B atoms, leaving the remaining one sp^2 orbital empty to accommodate the lone pair electrons from the ligand L. Each B atom has its p_z orbital singly occupied. Therefore, the $B_5L_5^-$ compounds have six π -electrons, satisfying the Hückel $4n + 2$ rule and thus could be expected with aromaticity. The calculated nucleus independent chemical shifts (NICS) at the points 1.5 Å above the B_5 ring centres are listed in the table S1 in SI. All the calculated NICS values are negative verifying their aromaticity. **1c** has the most negative NICS of -11.0 ppm.

Another factor determining the stability of $B_5L_5^-$ is the strength of their B–L bonds. Thus, we calculated the interaction energies (E_i) and

deformation energies (E_d) for the B–L bonds of **1a**–**1f**. These energies are defined as follows:

$$E_i = E_{B_5L_4^-} + E_L - E_{B_5L_5^-} \quad (1)$$

$$E_d = E_{B_5L_4, opt} + E_{L, opt} - E_{B_5L_5^-} \quad (2)$$

where $E_{B_5L_5^-}$, $E_{B_5L_4, opt}$ and $E_{L, opt}$ are the total energies of the correspondingly relaxed structures, and $E_{B_5L_4^-}$ and E_L are single point energies of $B_5L_4^-$ and L which maintain the same geometric structures as those in $B_5L_5^-$. In order to get reliable results, these energies are calculated using the hybrid functional M062X and B3LYP and the pure functional PBE at the 6-31G(d, p) level. The results calculated by M062X-D3BJ/6-31G(d, p) method are plotted in Fig. 2c. Among the six ligands, C can make the strongest B–L bond because of its larger E_d than those of B–F, which can be explained by the electron-donating property of methyl. This result is in well accordance with that **1c** has the strongest aromaticity. **B** has relatively weaker bonding affinities with the B_5^- rings because of its lowest E_i and E_d . The energies calculated by B3LYP-D3BJ/6-31G(d, p) and PBE-D3BJ/6-31G(d, p) methods are plotted in Figure S1 in the SI, which leads to the same results.

To analyse the B–L bonding property, we performed the ETS-NOCV calculations for **1a** and **1b** as the examples (Fig. 3). For either **1a** or **1b**, the orbital interaction between the $B_5L_4^-$ and L fragments are mainly contributed by two components: the σ -donation from L to $B_5L_4^-$ ($L \rightarrow B_5L_4^-$) and the π -back-donation ($L \leftarrow B_5L_4^-$). According to the decomposed orbital interaction energies (Fig. 3), the σ -donation is dominating in both cases. This bonding configuration agrees with those established for base stabilized borenates, in which the base also has π^* antibonding orbitals, and is consistent with the model of Fig. 1a [1,38–40]. Comparing **1a** and **1b**, the energy contributions of the σ -donations of **1a** and **1b** are -106.1 and -89.0 kcal mol $^{-1}$, respectively, in agreement with the relatively weaker coordination capability of N_2 than CO (Fig. 1c). We also conducted ETS-NOCV calculations for **1c**–**1f** and the results are presented in the SI (Figure S2 in SI).

3.2. Metallocene-like borene compounds

Drawing analogy with the experimentally achievable metallocene molecules, we constructed 30 metallocene-like compounds using the B_nL_n rings as the η^n ligands (Fig. 4). Among them, **2a**–**6c** are half-sandwich structures and **7a**–**11c** are sandwich structures. Ligand A (*i.e.*, CO) is used as the ligand coordinated with the boron rings because CO has moderate affinity with B_5^- ring and its small-size can avoid the intramolecular steric repulsion. For each structural group, **ma**, **mb** and **mc** ($m = 2 - 11$) have the same B_nL_n ($n = 3 - 7$) ring and three metals of the same group in the periodic table. **2a**–**6c** can be denoted as $[(\eta^n-B_nL_n)M(CO)_3]$, and **7a**–**11c** can be denoted as $[(\eta^n-B_nL_n)_2M]$, where M are the metals. These 30 compounds have one common feature: the central metal atoms all have 18 valance electrons.

To study the bonding affinity between the metal and B_nL_n rings, we calculated their E_i and E_d (Fig. 5). The definition of these energies are similar to those of equations (1) and (2). For **2a**–**6c** the two interaction fragments are the B_nL_n ring and $M(CO)_3$ cluster and those for **7a**–**11c** are B_nL_n ring and the $[(\eta^n-B_nL_n)_2M]$. For comparison, those of the experimentally synthesized compounds $[(\eta^5-Cp)Mn(CO)_3]$ (Cp = cyclopentadiene) and $[(\eta^5-Cp)_2Fe]$ are also calculated.

According to Fig. 5, the three-membered $\eta^3-B_3(CO)_3$ in **2** and **7** are the weakest coordination capability to metals. The E_i and E_d of **2** and **7** are lower than those of **3**–**6** and **8**–**11** and also lower than those of experimentally synthesized $[(\eta^5-Cp)Mn(CO)_3]$ and $[(\eta^5-Cp)_2Fe]$ (the dash lines in Fig. 5), which indicates their poor stabilities.

According to Fig. 5c and d, the $\eta^5-B_5(CO)_5$ ligand in **4** and **9** is the best candidate to stabilize metal or metal clusters. For the metals in the same period in the periodic table, the E_i and E_d of **4** and **9** are generally larger than those of the others. For the metals in the same group in the

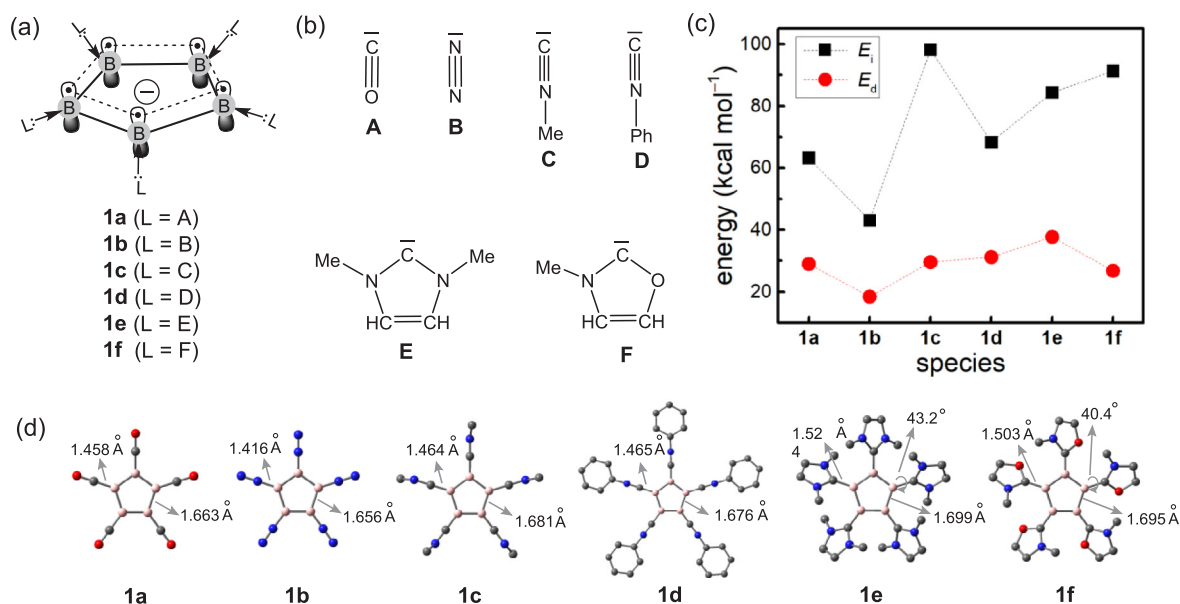


Fig. 2. (a) The electronic structure model of cyclic B_5^- complexes **1a**–**1f** that each has five donor–acceptor bonds and six π electrons. (b) Ligands making dative bonds with the cyclic B_5^- , in which the electron lone pairs are marked by short lines. Me, methyl; Ph, phenyl. (c) The calculated interaction energies (E_i) and deformation energies (E_d) for **1a**–**1f**. (d) The geometric structures of **1a**–**1f** with key bond lengths and dihedral angles labelled and the hydrogen atoms are omitted for clarity.

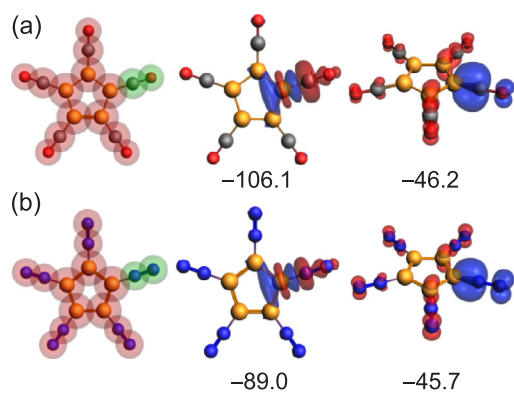


Fig. 3. Orbital interactions contributing the most to the bonding between CO and the rest of the structures of **1a** (A) and **1b** (B). For each structure, the left diagram defines the two interacting fragments; the middle and right are the NOCV differential densities (isovalue = 0.003 au) for the two strongest orbital interactions between the two fragments; the blue and red colors mean positive and negative electron densities, respectively; the electrons trans from the red areas to the blue areas; the energy contribution values are in kcal/mol.

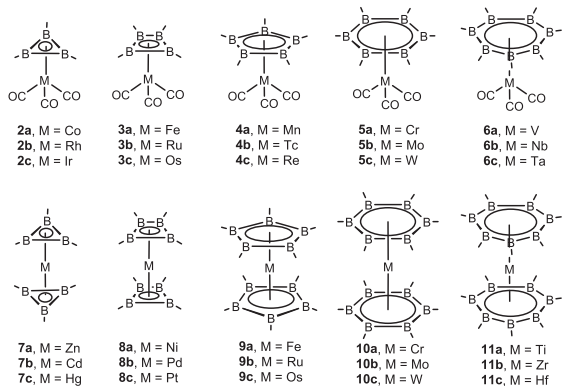


Fig. 4. Constructed half-sandwich and sandwich complexes based on 18-electron rule. The Lewis bases are A in all structures. All the base ligands linked to the boron atoms are not shown for clarity.

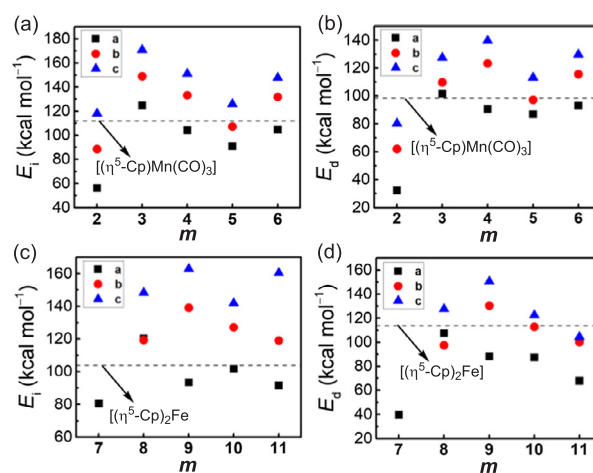


Fig. 5. The E_i and E_d in kcal mol⁻¹ for **2**–**6** (a and b) and **7**–**11** (c and d) calculated at the M062X-D3/6-31G(d, p) ~ SDD level of theory. The E_i and E_d for **7b** and **7c** are unavailable because of the convergence failure of geometric optimization.

periodic table, it is a general tendency that moving down the group, the atomic radii of the metals increases, and the E_i and E_d also increase. For instance, the E_i and E_d increase in the order of **4a** < **4b** < **4c**. This indicates the increasing trend of the bond strength moving down the group, which is similar to the recent study on the $[(\eta^6\text{-C}_6\text{H}_6)\text{M}(\text{CO})_3]$ where M = Cr, Mo and W [41].

Taking the dash lines, which stand for the E_i and E_d for the synthesized $[(\eta^5\text{-Cp})\text{Mn}(\text{CO})_3]$ and $[(\eta^5\text{-Cp})_2\text{Fe}]$, as references, some of the structures have comparable or larger E_i and E_d . These results may cast light on the future synthesis of our constructed structures. The energies calculated by B3LYP-D3BJ/6-31G(d, p) and PBE-D3BJ/6-31G(d, p) are plotted in Figure S3 and S4 in the SI, which leads to the same results.

3.3. Sandwich nanowire

The above results suggest that Lewis base stabilized boron rings B_nL_n can also strongly bond with metals to form the metallocene-like

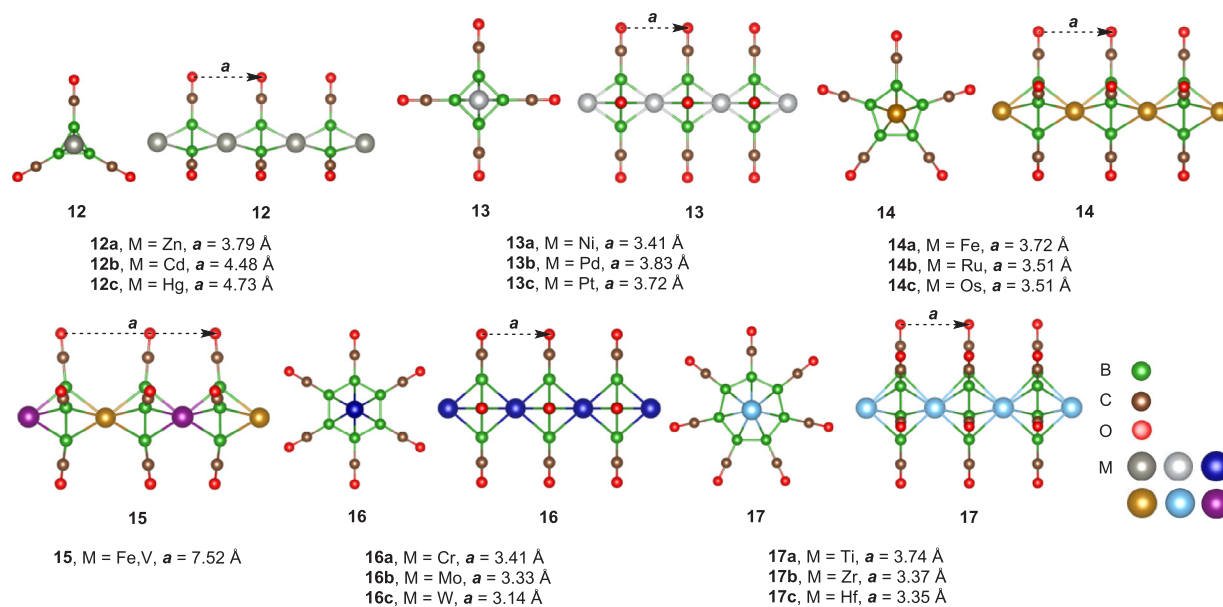


Fig. 6. Geometric structures for the extended 1D nanowires 12 – 17. The metal species and the corresponding lattice parameter a are labelled.

half-sandwich and sandwich structures. And recently, one dimensional multidecker V_nBz_{n+1} ($Bz = \text{benzene}$) sandwich complexes have been synthesized, and some have been predicted to be organic half-metals [42–45]. This encourages us to construct the 1D nanowires based on B_nL_n and transition metals. We extended the 0D molecules **7a** – **11c** to 1D nanowires **12a** – **17c** (Fig. 6). For these sandwich nanowires, both eclipsed and staggered configurations are possible. Only the eclipsed configuration was considered here because of the similar total energies of these two configurations (within 0.02 eV per Cp ring [46]). To consider different magnetic states, supercells containing four primitive cells were used for the calculations. All the structures were optimized without symmetry constraints. After geometry optimization, no significant structural distortion was observed. Fig. 6 presents the geometric structures for these nanowires with the optimal lattice parameters a labelled. For each structure, the energy difference between the FM state and the AFM state is listed in Table S2 of the SI. The total magnetic moment per unit cell and the localized magnetic moment on the metal atoms of the ground states are also listed. For all the examined sandwich nanowires, the FM states have slightly lower energies than the corresponding AFM states and thus are the ground states.

In 2008, Lu and co-workers reported the similar 1D sandwich nanowires consisting of vanadium (V), Fe, Cp, and Bz [46]. The $(VCp)_\infty$ and $(VBzVcP)_\infty$ wires are predicted to be organic half-metals which can realize 100% spin polarization transportation and thus is intriguing for organic spintronics. In order to get an insight into the electronic structures of the nanowires based on B_nL_n , we calculated the electronic band structures for **12a** – **17c**. Taking **14a**, i.e., $[B_5(CO)_5Fe]_\infty$ as the example, its FM state is the ground state, but is energetically lower than the AFM state by only 3 meV per $B_5(CO)_5Fe$. Fig. 7a and b display the band structures for its FM and AFM states, respectively. For the FM state, both of the majority and minority spin have metallic nature with a doubly degenerate band crossing the Fermi level (E_f). But for the AFM state, the majority spin has a semiconducting nature with a direct band gap of 0.32 eV, meanwhile the minority spin also has a direct band gap of 0.05 eV. Thus, $[FeB_5(CO)_5]_\infty$ is an organic metal in FM state but a semiconductor in AMF state.

Inspired by Lu's work, we displaced one Fe with V and constructed **15**, i.e., $[VB_5(CO)_5FeB_5(CO)_5]_\infty$ nanowire. As shown in Fig. 6, the $B_5(CO)_5$ rings are arranged unevenly in **15**, agreeing with the different atomic radii of Fe and V. Also, the FM state is the ground state. The band structure and the projected density of states (PDOS) of FM **15** are

shown in Fig. 7c and d, respectively. Its majority spin of has a semiconducting nature with a direct band gap of 1.33 eV, whereas the minority spin is metallic. Thus **15** is an organic half-metal. According to the PDOS in Fig. 7d, in the majority part, the bands near E_f are mainly derived from the 3d orbitals of the V atom and the 2p orbitals of the B atom. While in the minority part, the bands near E_f are mainly derived from the 3d orbitals of the Fe atom. The total magnetic moment of **15** is 5.29 μ_B per unit cell. The localized magnetic moment is 2.27 μ_B on V, 3.68 μ_B on Fe and $-0.33 \mu_B$ per $B_5(CO)_5$ ring. The low capability to accept electrons form π -orbital of boron ring is vital for opening a band gap in the majority spin part of the nanowire and finally leads to its half-metal nature.

To evaluate the stabilities of **15**, which is an organic half-metal and has promising application in spintronics, we conducted 2 ps molecular dynamic (MD) simulations at 300 K, 500 K, 1000 K and 1500 K. According to the snapshots taken from the MD trajectories at 400 fs, 800 fs, 1200 fs, 1600 fs and 2000 fs (Figure S5 in the SI), no obvious bond cleavages appeared at 300 K, 500 K and 1000 K although crinkles existed. Only at higher temperatures of 1500 K, the deformation of boron ring occurred. These MD simulations suggest that **15a** can survive at considerably high temperatures.

4. Conclusions

Lewis base stabilized $B_5L_5^-$ compounds have six π -electrons and thus possess aromaticity. Among the six ligands L studied, the acetonitrile C has the strongest coordination capability to B^5- ring thus forms the strongest B–L donor acceptor bonds. The $B_5(CO)_5$ rings have comparable or even stronger coordination capabilities than cyclopentadiene when forming the half-sandwich and sandwich metallocene-like molecules with transition metals. Further construction and computation of 1D nanowires based on these $B_5L_5^-$ and transition metals suggest that the sandwich nanowires can have intriguing spin properties. For example, $[FeB_5(CO)_5]_\infty$ is metallic in its FM state but semiconducting in its AMF state, and the hybrid $[VB_5(CO)_5FeB_5(CO)_5]_\infty$ wire is an organic half-metal. The results suggest the opportunity to design metallocene-like molecules and nanowires with intriguing electronic properties based on Lewis base stabilized borynes, which may greatly expand the application of such peculiar borons.

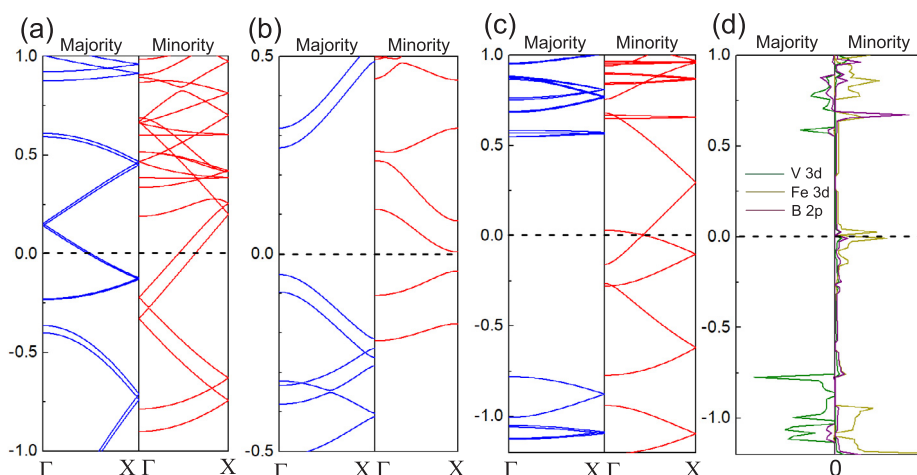


Fig. 7. Spin-resolved band structures of **14a** in the FM (a) and AFM (b) state and **15** in AFM (c) state. The spin-resolved local density of states of **15** in the AFM, i.e. the ground-state, is shown in panel (d).

CRediT authorship contribution statement

Xiaojie Fu: Data curation, Investigation, Writing - original draft. **Di Wang:** Investigation. **Xiaolin Song:** Investigation. **Xingfa Gao:** Supervision. **Joonkyung Jang:** Writing - review & editing. **Xuejiao J. Gao:** Project administration, Writing - review & editing.

Declaration of Competing Interest

The authors declare that they have no known competing financial interests or personal relationships that could have appeared to influence the work reported in this paper.

Acknowledgment

This work was supported by the NSFC Project 21773095 and 21907043. This paper was also supported by the Brain Pool Project of the MEST (Ministry of Education, Science and Technology) and by the National Research Foundation of Korea Grant funded by the Korean Government (No. NRF-2015R1A2A2A01004208).

Appendix A. Supplementary data

Supplementary data to this article can be found online at <https://doi.org/10.1016/j.cplett.2020.137336>.

References

- [1] L. Zhao, M. Hermann, N. Holzmann, G. Frenking, Dative Bonding in Main Group Compounds, *Coord. Chem. Rev.* 344 (2017) 163–204.
- [2] G. Frenking, M. Hermann, D.M. Andrada, N. Holzmann, Donor-Acceptor Bonding in Novel Low-Coordinated Compounds of Boron and Group-14 Atoms C-Sn, *Chem. Soc. Rev.* 45 (2016) 1129–1144.
- [3] P.P. Power, Main-Group Elements as Transition Metals, *Nature* 463 (2010) 171.
- [4] G. Frenking, N. Fröhlich, The Nature of the Bonding in Transition-Metal Compounds, *Chem. Rev.* 100 (2000) 717–774.
- [5] Y. Wang, G.H. Robinson, N-Heterocyclic Carbene—Main-Group Chemistry: A Rapidly Evolving Field, *Inorg. Chem.* 53 (2014) 11815–11832.
- [6] H. Braunschweig, R.D. Dewhurst, Boron-Boron Multiple Bonding: From Charged to Neutral and Back Again, *Organometallics* 33 (2014) 6271–6277.
- [7] T.T. Ba, N.M. Tho, Boron-Boron Multiple Bond in [B(NHC)]₂: Towards Stable and Aromatic [B(NHC)]₂ N Rings, *Angew. Chem. Int. Ed.* 52 (2013) 4554–4557.
- [8] J. Jin, G. Wang, M. Zhou, D.M. Andrada, M. Hermann, G. Frenking, The [B₂(NN)₃]⁺ and [B₂(CO)₃]⁺ Complexes Featuring the Smallest π-Aromatic Species B³⁺, *Angew. Chem. Int. Ed.* 55 (2016) 2078–2082.
- [9] Y. Wang, B. Quillian, P. Wei, C.S. Wannere, Y. Xie, R.B. King, H.F. Schaefer, P.v.R. Schleyer, G.H. Robinson, A Stable Neutral Diborene Containing a B₂ Double Bond, *J. Am. Chem. Soc.* 129 (2007) 12412–12413.
- [10] R. Kinjo, B. Donnadieu, M.A. Celik, G. Frenking, G. Bertrand, Synthesis and Characterization of a Neutral Tricoordinate Organoboron Isoelectronic with Amines, *Science* 333 (2011) 610–613.
- [11] H. Braunschweig, R.D. Dewhurst, F. Hupp, M. Nutz, K. Radacki, C.W. Tate, A. Vargas, Q. Ye, Multiple Complexation of Co and Related Ligands to a Main-Group Element, *Nature* 522 (2015) 327.
- [12] H. Braunschweig, I. Krummenacher, M.-A. Légaré, A. Matler, K. Radacki, Q. Ye, Main-Group Metallomimetics: Transition Metal-Like Photolytic Co Substitution at Boron, *J. Am. Chem. Soc.* 139 (2017) 1802–1805.
- [13] D. Fatme, M. David, S.D. W. G. Bertrand, Synthesis and Reactivity of a CAAC–Aminoborylene Adduct: A Hetero-Allene or an Organoboron Isoelectronic with Singlet Carbenes, *Angew. Chem. Int. Ed.* 53 (2014) 13159–13163.
- [14] A., C. P.; C., W. G.; Titel, J.; W., S. D., Metal-Free Catalytic Hydrogenation. *Angew. Chem. Int. Ed.* 46 (2007) 8050–8053.
- [15] S. Patrick, S. Sina, L. Stefanie, K. Gerald, F. Roland, E. Gerhard, Metal-Free Catalytic Hydrogenation of Enamines, Imines, and Conjugated Phosphinoalkenylboranes, *Angew. Chem. Int. Ed.* 47 (2008) 7543–7546.
- [16] B. Su, R. Kinjo, Construction of Boron-Containing Aromatic Heterocycles, *Synthesis-Stuttgart* 49 (2017) 2985–3034.
- [17] M.-A. Légaré, G. Bélanger-Chabot, R.D. Dewhurst, E. Welz, I. Krummenacher, B. Engels, H. Braunschweig, Nitrogen Fixation and Reduction at Boron, *Science* 359 (2018) 896–900.
- [18] X. Gao, X.J. Gao, Metal-Like Boronic–Organic Frameworks: A Design and Computation, *Inorg. Chem.* 56 (2017) 2490–2495.
- [19] W.J. Hehre, R. Ditchfield, J.A. Pople, Self-Consistent Molecular Orbital Methods. Xii. Further Extensions of Gaussian-Type Basis Sets for Use in Molecular Orbital Studies of Organic Molecules, *J. Chem. Phys.* 56 (1972) 2257–2261.
- [20] P.C. Hariharan, J.A. Pople, The Influence of Polarization Functions on Molecular Orbital Hydrogenation Energies, *Theor. Chim. Acta* 28 (1973) 213–222.
- [21] X. Cao, M. Dolg, Valence Basis Sets for Relativistic Energy-Consistent Small-Core Lanthanide Pseudopotentials, *J. Chem. Phys.* 115 (2001) 7348–7355.
- [22] X. Cao, M. Dolg, Segmented Contraction Scheme for Small-Core Lanthanide Pseudopotential Basis Sets, *THEOCHEM* 581 (2002) 139–147.
- [23] M.J. Frisch, et al., Gaussian 09, Gaussian Inc., Wallingford, CT, USA, 2009.
- [24] M.P. Mitoraj, A. Michalak, T. Ziegler, A Combined Charge and Energy Decomposition Scheme for Bond Analysis, *J. Chem. Theory Comput.* 5 (2009) 962–975.
- [25] L. Zhao, M. Hermann, W.H.E. Schwarz, G. Frenking, The Lewis Electron-Pair Bonding Model: Modern Energy Decomposition Analysis, *Nature Rev. Chem.* 3 (2019) 48–63.
- [26] L. Zhao, M. Hopffgarten, D.M. Andrada, Frenking, Gernot, Energy decomposition analysis, *WIRE: Comput. Mol. Science.* 8 (2018) e1345.
- [27] J.P. Perdew, Density-Functional Approximation for the Correlation Energy of the Inhomogeneous Electron Gas, *Physical Review B* 33 (1986) 8822–8824.
- [28] J.P. Perdew, Erratum: Density-Functional Approximation for the Correlation Energy of the Inhomogeneous Electron Gas, *Phys. Rev. B* 34 (1986) 7406.
- [29] A.D. Becke, Density-Functional Exchange-Energy Approximation with Correct Asymptotic Behavior, *Phys. Rev. A* 38 (1988) 3098–3100.
- [30] G. Velde, F.M. Bickelhaupt, E.J. Baerends, C. Fonseca Guerra, S.J.A. van Gisbergen, J.G. Snijders, T. Ziegler, Chemistry with Adf, *J. Comput. Chem.* 22 (2001) 931–967.
- [31] G. Kresse, J. Furthmüller, Efficient Iterative Schemes for Ab Initio Total-Energy Calculations Using a Plane-Wave Basis Set, *Physical Review B* 54 (1996) 11169–11186.
- [32] G. Kresse, D. Joubert, From Ultrasoft Pseudopotentials to the Projector Augmented-Wave Method, *Physical Review B* 59 (1999) 1758–1775.
- [33] J.P. Perdew, K. Burke, M. Ernzerhof, Generalized Gradient Approximation Made Simple, *Phys. Rev. Lett.* 77 (1996) 3865–3868.
- [34] H.J. Monkhorst, J.D. Pack, Special Points for Brillouin-Zone Integrations, *Physical Review B* 13 (1976) 5188–5192.
- [35] X.-W. Li, Y. Xie, P.R. Schreiner, K.D. Gripper, R.C. Crittendon, C.F. Campana, H.F. Schaefer, G.H. Robinson, Cyclogallanes and Metalloaromaticity. Synthesis and

- Molecular Structure of Dipotassium Tris((2,6-Dimesitylphenyl)Cyclogallene), $K_2[(Mes_2C_6H_3)Ga]_3$ (Mes = 2,4,6-Me₃C₆H₂): A Structural and Theoretical Examination, *Organometallics* 15 (1996) 3798–3803.
- [36] X.-W. Li, W.T. Pennington, G.H. Robinson, Metallic System with Aromatic Character. Synthesis and Molecular Structure of $Na_2[(2,4,6-Me_3C_6H_2)_2C_6H_3]Ga_3$ the First Cyclogallane, *J. Am. Chem. Soc.* 117 (1995) 7578–7579.
- [37] J., W. R., Marcin, B., P., P. P., Synthesis and Structure of the “Dialuminyne” $Na_2[Ar'AlAlAr']$ and $Na_2[(Ar''Al)_3]$: Al□Al Bonding in Al_2Na_2 and Al_3Na_2 Clusters, *Angew. Chem. Int. Ed.* 45 (2006) 5953–5956.
- [38] S. Morisako, R. Shang, Y. Yamamoto, H. Matsui, M. Nakano, Triaminotriborane(3): A Homocatenated Boron Chain Connected by B-B Multiple Bonds, *Angew. Chem. Int. Ed.* 56 (2017) 15234–15240.
- [39] F. Gernot, Dative Bonds in Main-Group Compounds: A Case for More Arrows!, *Angew. Chem. Int. Ed.* 53 (2014) 6040–6046.
- [40] M.A. Celik, R. Sure, S. Klein, R. Kinjo, G. Bertrand, G. Frenking, Borylene Complexes (BH)L₂ and Nitrogen Cation Complexes (N⁺)L₂: Isoelectronic Homologues of Carbones Cl₂, *Chem. Eur. J.* 18 (2012) 5676–5692.
- [41] J. Böhnke, H. Braunschweig, J.O.C. Jiménez-Halla, I. Krummenacher, T.E. Stennett, Half-Sandwich Complexes of an Extremely Electron-Donating, Redox-Active H6-Diborabenzene Ligand, *J. Am. Chem. Soc.* 140 (2018) 848–853.
- [42] T. Kurikawa, H. Takeda, M. Hirano, K. Judai, T. Arita, S. Nagao, A. Nakajima, K. Kaya, Electronic Properties of Organometallic Metal–Benzene Complexes [Mn(Benzene)M (M = Sc–Cu)], *Organometallics* 18 (1999) 1430–1438.
- [43] K. Miyajima, K. Muraoka, M. Hashimoto, T. Yasuike, S. Yabushita, A. Nakajima, K. Kaya, Quasi-Band Electronic Structure of Vn(Benzene)N + 1 Clusters, *J. Phys. Chem. A* 106 (2002) 10777–10781.
- [44] K. Miyajima, A. Nakajima, S. Yabushita, M.B. Knickelbein, K. Kaya, Ferromagnetism in One-Dimensional Vanadium–Benzene Sandwich Clusters, *J. Am. Chem. Soc.* 126 (2004) 13202–13203.
- [45] K. Miyajima, S. Yabushita, M.B. Knickelbein, A. Nakajima, Stern–Gerlach Experiments of One-Dimensional Metal–Benzene Sandwich Clusters: Mn(C₆H₆)M (M = Al, Sc, Ti, and V), *J. Am. Chem. Soc.* 129 (2007) 8473–8480.
- [46] L. Wang, et al., Novel One-Dimensional Organometallic Half Metals: Vanadium-Cyclopentadienyl, Vanadium-Cyclopentadienyl-Benzene, and Vanadium-Anthracene Wires, *Nano Lett.* 8 (2008) 3640–3644.